TECTONIC MAPPING OF RIFT ZONES ON RHEA, TETHYS, AND DIONE

P. K. Byrne[1], P. M. Schenk[1], and P. J. McGovern[1].
[1]Lunar and Planetary Institute, Universities Space Research Association, Houston, TX 77058 (byrne@lpi.usra.edu).

- **Large rifts occur on each moon, increasing in tectonic complexity from Rhea, to Tethys, to Dione**
- **Rifting is oriented ~N–S, concentrated within or bordering these bodies' trailing hemispheres**
- **The pattern of deformation is similar despite differences in satellite size and interior structure**

Introduction: Rhea, Tethys, and Dione are among the largest moons of Saturn. Each exhibits substantial extensional tectonic deformation in the form of rift zones (termed chasmata). With a radius of 561 km, Dione is likely primarily composed of water ice but may have a silicate core. Tethys is 531 km in radius and is composed almost entirely of water ice. Rhea has a radius of 764 km and consists primarily of water ice, but whether this moon is differentiated is unknown [1].

A wide variety of sources of stress has been proposed to account for the surface deformation of icy satellites, both within and beyond the Saturnian system. These stresses can be classified as either endogenic (inherent to the body) or exogenic (originating from beyond the body). Endogenic sources of stress include changes in volume due to phase changes within a satellite and solid-state convection (e.g., [2,3]). Exogenic stresses may arise from processes including polar wander, diurnal tides, non-synchronous rotation (NSR), and tidal recession (e.g., [4–9]).

Despite differences in the geophysical properties of these bodies, and the varying degrees to which these processes are applicable to a given moon, that there are broad similarities in how extensional strains are manifest across all three bodies suggests some commonality in the origin and magnitudes of the causal stresses. It may be, therefore, that some process (or combination of processes) has operated on each of these three moons independent of local geological and dynamical conditions.

Here, we perform structural mapping of the prominent extensional systems on Rhea, Tethys, and Dione, using the most recent global photomosaics and digital terrain models (DTMs) available for each moon. Our mapping results serve as inputs for spherical finite-element models with which we explore the process(es) responsible, and parameters required, for the strains we observe on these icy moons.

Methods: We use global photomosaics of each moon derived from Cassini Imaging Science Subsystem (ISS) data, which include new albedo models and the highest resolution color images to date. Our global topographic products are combined from stereophotogrammetry- and photoclinometry-derived DTMs. We have generated photomosaics at effective resolutions of 400 m/px for Rhea, and at 250 m/px for Tethys and Dione. Our global DTMs of Rhea, Tethys, and Dione have resolutions of 1,000 m/px, 500 m/px, and 400 m/px, respectively. Within ArcGIS, we record the surface traces of tectonic landforms, document morphometrics such as overlap between individual fault segments, and estimate strains across select structures and the chasmata in general.

Rift Zone Distributions: The distributions of the chasmata on Rhea, Tethys, and Dione, are shown

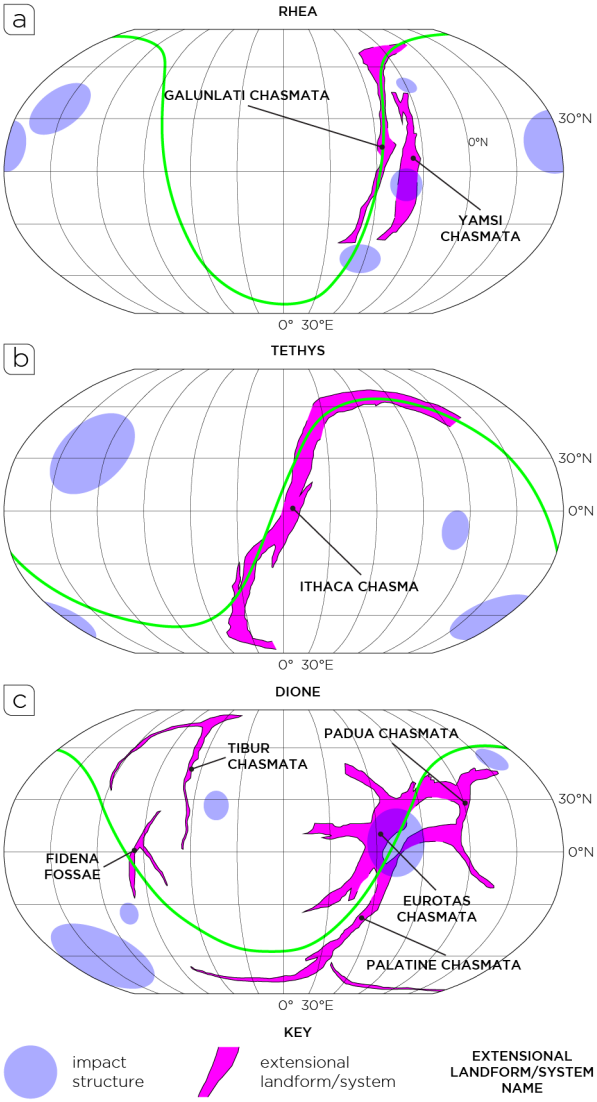

Fig. 1. Schematic maps of the chasmata on (**a**) Rhea, (**b**) Tethys, and (**c**) Dione, in Robinson projections centered at 0°E.

Rhea. Galunlati and Yamsi Chasmata are both located close to the center of Rhea's trailing hemisphere (**Fig. 1a**), and trend approx. N–S. Galunlati is the longer of two, extending for ~1,500 km and subtending 113° of arc. Both systems vary in width along their course, from ~40–90 km, and are characterized by normal fault segments that display minor local variations in strike, relay ramps, and numerous stepover regions tens of kilometers long.

Tethys. Tectonic deformation on this moon is dominated by Ithaca Chasma, which ranges from high northern latitudes in the moon's trailing hemisphere, across the prime meridian, to high southern latitudes at the perimeter of the leading hemisphere (**Fig. 1b**). Although at 1,400 km it is shorter than the chasmata on Rhea, Ithaca Chasma subtends a longer arc (151°), and is between 70 km and 110 km in width. Ithaca Chasma hosts more individual fault segments than either chasma on Rhea, but is similarly oriented ~N–S along much of its course.

Dione. Rifting on this moon displays the greatest structural complexity of the three Saturnian bodies we survey. Several chasmata populate the center of Dione's trailing hemisphere, with several following again ~N–S-oriented trends (notably Palatine, Eurotas, and Padua Chasmata) (**Fig. 1c**). Collectively, these rifts extend ~1,300 km, subtend 133° of arc, and vary in width from 40 km to 130 km. The cumulative number of individual fault segments on Dione is substantially greater than that of Rhea or Tethys.

Titania. We have also considered the extensional landforms on Titania, the largest moon of Uranus. With a radius of 788 km, Titania is similar in size to Rhea, although Titania is the denser of the two and may be differentiated [10]. Titania hosts two chasmata, Messina and Belmont, at least parts of which are situated near the sub-Uranus point and which trend approx. N–S (**Fig. 2**). With less than 35% of Titania's surface imaged, however, the full extent of Messina

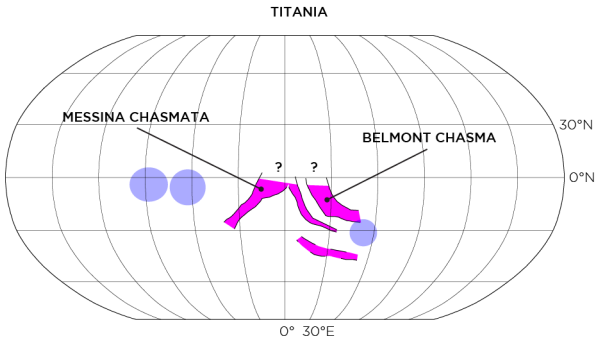

Fig. 2. Schematic map of the known chasmata on Titania. Symbology, colors, and projection for this map are as for those in **Fig. 1**.

Discussion: Despite differences in size, density, internal structure, impact cratering history, and dynamical environment, fundamental similarities exist in the style and distribution of large-scale extensional deformation on the icy satellites we investigate. Rifting is concentrated within or at the borders of each moon's trailing hemisphere, shows a preference for ~N–S-oriented strikes, and appears to show a systematic increase in complexity from Rhea, to Tethys, to Dione.

Moreover, sections of each moon's chasma or chasmata appear to lie along substantial portions of great circles (green lines in **Fig. 1a–c**), indicating that the process(es) responsible for rifting operated over considerable distances along lines of constant bearing (in spherical geometry). The concentration of strain into narrow but laterally extensive regions has also been documented, for example, on Mercury [11], Venus [12], and Mars [13]. We note, too, that tidally induced stresses alone tend to result in degree-two distributions in strain, in contrast to the hemispherical dichotomy in the localization of strain observed on these three Saturnian icy satellites. It may be then that these large-scale rifts formed under a scenario in which tidal processes contributed at most a secondary component of stress, with Rhea representing the least, and Dione the most advanced stage of deformation.

Outlook: In addition to continued quantitative structural mapping, we are also calculating models of stresses in the icy shells of Rhea, Tethys, and Dione using the finite-element COMSOL Multiphysics code. With COMSOL, we consider spherical geometries in fully three-dimensional simulations, as well as time-dependent stress histories resulting from sequential events in the evolution of icy satellites (e.g., despinning followed by polar wander) where the failure that one mechanism induces leaves a decidedly non-uniform starting stress state for the second mechanism.

References: [1] Thomas, P. C. et al. (2007) *Icarus*, *190*, 573–584. [2] Hillier, J. and Squyres, S. W. (1991) *JGR*, *96*, 15,665–15,674. [3] Czechowski, L. and Leliwa-Kopystyńskia, J. (2002) *Adv. Space Res.*, *29*, 751–756. [4] Nimmo, F. (2004) *JGR*, *109*, E01003. [5] Nimmo, F. and Matsuyama, I. (2007) *GRL*, *34*, L19203. [6] Matsuyama, I., and Nimmo, F. (2008) *Icarus*, *195*, 459–473. [7] Nimmo, F. and Manga, M. (2009) in *Europa*, Pappalardo, R. T. et al. (eds.) Univ. Arizona Press, pp. 381–404. [8] Patthoff, D. A. et al. (2012) *LPS*, *43*, Abstract 2527. [9] Martin, E. S. and Kattenhorn, S. A. (2014) *LPS*, *45*, Abstract 1083. [10] Hussmann, H. et al. (2006) *Icarus*, *185*, 258–273. [11] Byrne, P. K. et al. (2014) *Nature Geosci.*, *7*, 301–307. [12] Zuber, M. T. and Parmentier, E. M. (2002) *Nature*, *377*, 704–707. [13] Wilson, L. and Head, J. W. (2002) *JGR*, *107*, E8, 1-1–1-24.